Fundamental Limits for Joint Relative Position and Orientation Estimation with Generic Antennas

Robert Pöhlmann, Siwei Zhang, Armin Dammann
German Aerospace Center (DLR)
Institute of Communications and Navigation
Oberpfaffenhofen, 82234 Wessling, Germany
Email: {Robert.Poehlmann, Siwei.Zhang, Armin.Dammann}@dlr.de

Peter A. Hoeher
University of Kiel
Faculty of Engineering
24143 Kiel, Germany
Email: ph@tf.uni-kiel.de

***Abstract*—Automated multi-agent robotic systems are a promising technology for extra-terrestrial exploration. Autonomous control of such systems requires position as well as orientation awareness. Having a multi-port antenna system like an antenna array or a multi-mode antenna (MMA) installed on each agent, position and orientation can be estimated when the agents cooperatively communicate via radio signals. The aim of this paper is to derive the fundamental limits for relative, i.e. anchor-free, joint position and orientation estimation. Using wavefield modeling and manifold separation, the inclusion of calibration data from real multi-port antenna systems is possible. The Cramér-Rao bound (CRB) is derived directly on the received signal, thus representing a fundamental limit. We then use the derived bound to analyze the position and orientation estimation capabilities of a multi-agent system employing MMAs.**

I. Introduction

Multi-agent robotic systems are a promising approach to fulfill challenging tasks like terrestrial surveillance and disaster management as well as extra-terrestrial exploration. For autonomous operation, we need both communication between the agents and a reliable navigation solution. On earth, a global navigation satellite system (GNSS) can be used in many scenarios. However, GNSS signal reception can be blocked or impaired. For most extra-terrestrial missions, GNSS is not an option. A combined communication and navigation system has been investigated in [1]. However, it only provides the position of the agents. In order to generate control commands, e.g. to achieve a mission goal while keeping a favorable formation [2], the orientation of the agents must be known as well. Consequently, we investigate fundamental limits in terms of the Cramér-Rao bound (CRB) for joint relative position and orientation estimation.

In this paper we consider a combination of time-of-arrival (ToA) and direction-of-arrival (DoA). For ToA, the signal propagation time, or time-of-flight, between agents is measured to obtain a range estimate. Usually we are dealing with non-synchronized networks, so two-way ranging, also called round-trip delay, is performed. The DoA of a signal can be determined by employing a multi-port antenna system like an antenna array or a multi-mode antenna (MMA) [3], [4]. DoA estimation provides angle information, thus enabling orientation estimation and improving positioning.

Cooperative positioning refers to collaborating agents for the purpose of positioning. Shen *et al.* have derived bounds for anchored cooperative positioning [5]. The anchor-free case is analyzed in [6]. Dynamic scenarios are treated by Popescu *et al.* in terms of the posterior CRB [7]. Less literature can be found on the topic of joint position and orientation estimation. Bounds for the single link case have been derived in [8], [9]. An extensive framework for fundamental limits regarding non-cooperative networks having anchors is provided in [10], where also the benefits of cooperation are analyzed. Usually ideal antenna arrays like uniform linear array (ULA) or uniform circular array (UCA) are assumed.

This paper derives the CRB for anchor-free joint position and orientation estimation for generic antennas, allowing the inclusion of real antenna calibration or electromagnetic field (EMF) simulation data. A closed-form expression for the CRB is obtained by applying wavefield modeling and manifold separation [11]. The derivation is done directly based on the received signal waveforms instead of extracted signal metrics. Like that, all information contained in the signal is taken into account and the resulting bounds provide fundamental limits for the position and orientation accuracy. The CRB is then used to assess the position and orientation estimation performance of a multi-agent system employing MMAs.

II. Cramér-Rao Bound Derivation

A. System & Signal Model

The scenario and the basic metrics can be seen in Figure 1. Accordingly, the range between two agents i and j is given by

$$c\tau_{i,j} = ||\boldsymbol{p}_j - \boldsymbol{p}_i||, \tag{1}$$

with the speed of light c, the signal propagation time $\tau_{i,j}$, the Euclidean norm $||.||$ and the position of agent i, $\boldsymbol{p}_i = \begin{bmatrix} x_i & y_i \end{bmatrix}^T$. The DoA of the signal measured in the body frame of the agent i is given by

$$\theta_{i,j} = \theta'_{i,j} - \psi_i = \arctan2\left(y_j - y_i,\, x_j - x_i\right) - \psi_i, \tag{2}$$

where $\arctan2(y, x)$ is the four-quadrant inverse tangent and ψ_i is the orientation of agent i.

We assume that the signals are transmitted with a single omni-directional antenna. On the receive side, we assume a

ISBN 978-90-827970-1-5

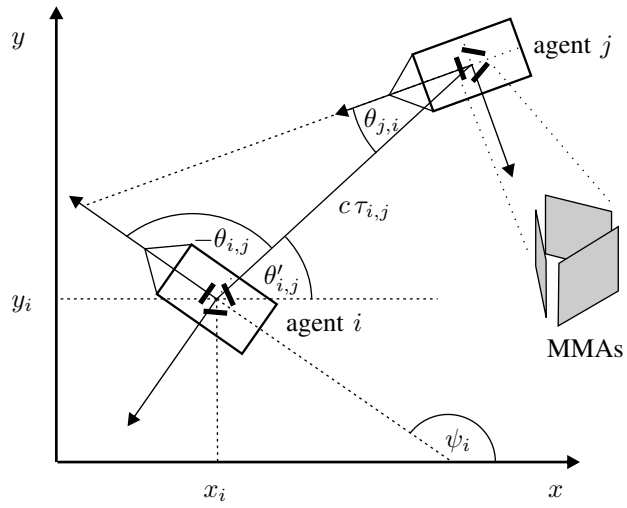

Fig. 1. Geometry of the problem. The illustration shows two agents i and j, the range in between $c\,\tau_{i,j}$, the DoAs $\theta_{i,j}$ and $\theta_{j,i}$ and the position $\boldsymbol{p}_i = [x_i\ y_i]^T$ and orientation ψ_i of agent i.

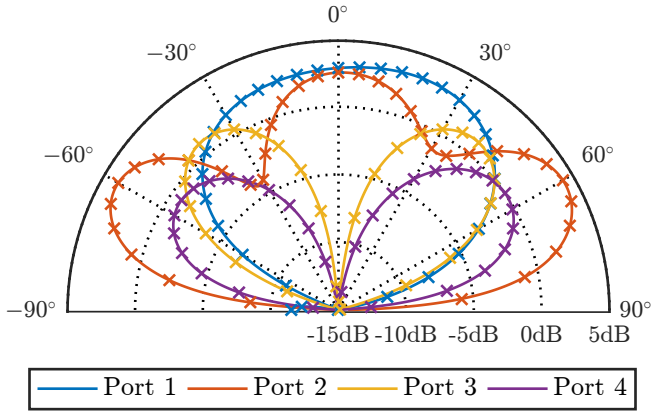

Fig. 2. Sampled (crosses) and interpolated (solid lines) MMA power pattern.

generic multi-port antenna system with M ports. In Section III, we present results for an MMA. The signal received by agent i on antenna port m from transmitting agent j is given by

$$r^m_{i,j}(n) = \alpha_{i,j} e^{\mathrm{j}\phi_{i,j}}\, a^m(\theta_{i,j})\, s(nT - \tau_{i,j}) + w^m_{i,j}(n), \quad (3)$$

with real amplitude $\alpha_{i,j}$, phase offset between transmitter and receiver $\phi_{i,j}$, sampled, delayed reference signal $s(nT-\tau_{i,j})$ with sample index $n = 0, ..., N-1$ and sample period T. The noise $w^m_{i,j}(n)$ is white circular symmetric normal distributed with variance σ^2. $a^m(\theta_{i,j})$ is one coefficient of the antenna response vector $\boldsymbol{a}(\theta_{i,j}) = [a^0(\theta_{i,j}), ..., a^{M-1}(\theta_{i,j})]^T$, which contains both gain and phase information and is assumed to be frequency independent. With free-space path loss, the amplitude is given by

$$\alpha_{i,j} = \frac{c\sqrt{P_{\mathrm{tx}}}}{4\pi f_c ||\boldsymbol{p}_j - \boldsymbol{p}_i||}, \quad (4)$$

for carrier frequency f_c and transmit power P_{tx}. We assume an orthogonal frequency-division multiplexing (OFDM) signal

$$s(nT - \tau_{i,j}) = \frac{1}{\sqrt{N_{\mathrm{sc}}}} \sum_{n_{\mathrm{sc}}=\lfloor -\frac{N_{\mathrm{sc}}-1}{2} \rfloor}^{\lfloor \frac{N_{\mathrm{sc}}-1}{2} \rfloor} S_{n_{\mathrm{sc}}} e^{\mathrm{j}2\pi n_{\mathrm{sc}} f_{\mathrm{sc}}(nT-\tau_{i,j})}, \quad (5)$$

with complex symbol $S_{n_{\mathrm{sc}}}$, N_{sc} subcarriers and subcarrier spacing f_{sc} [12].

In total there are L links between K agents, stored in the set $\mathbb{L} = \{..., (i,j), ...\}$. A specific agent i can receive signals from its neighbors $\mathbb{L}_i = \{..., j, ...\}$. With M antenna ports per agent and L links, the vector containing all measurements of the network at time index n is given by

$$\boldsymbol{r}(n) = \begin{bmatrix} ... & r^0_{i,j}(n) & ... & r^{M-1}_{i,j}(n) & ... \end{bmatrix}^T \in \mathbb{C}^{ML}. \quad (6)$$

The unknowns to be estimated for every agent i are its position and orientation,

$$\boldsymbol{\xi}_i = \begin{bmatrix} x_i & y_i & \psi_i \end{bmatrix}^T, \quad (7)$$

which are then stacked into the vector of agent unknowns

$$\boldsymbol{\xi} = \begin{bmatrix} \boldsymbol{\xi}_1^T & ... & \boldsymbol{\xi}_i^T & ... & \boldsymbol{\xi}_K^T \end{bmatrix}^T \in \mathbb{R}^{3K}. \quad (8)$$

Accordingly for every link, the amplitude $\alpha_{i,j}$ and phase $\phi_{i,j}$ are unknown,

$$\boldsymbol{\eta}_{(i,j)} = \begin{bmatrix} \alpha_{i,j} & \phi_{i,j} \end{bmatrix}^T, \quad (9)$$

thus for all links we get the vector of link unknowns

$$\boldsymbol{\eta} = \begin{bmatrix} ... & \boldsymbol{\eta}^T_{(i,j)} & ... \end{bmatrix}^T = \begin{bmatrix} ... & \alpha_{i,j} & \phi_{i,j} & ... \end{bmatrix}^T \in \mathbb{R}^{2L}, \quad (10)$$

which we treat as nuisance parameters.

B. Antenna Model

In order to obtain generic bounds for arbitrary antennas and to take the characteristics of real multi-port antenna systems into account, we apply an approach called wavefield modeling and manifold separation [11], [13]. The idea is to decompose the antenna response vector of the multi-port antenna system

$$\boldsymbol{a}(\theta_{i,j}) = \boldsymbol{G}\, \boldsymbol{\Psi}(\theta_{i,j}) \quad (11)$$

as the product of a sampling matrix $\boldsymbol{G} \in \mathbb{C}^{M \times U}$ and an orthonormal basis vector $\boldsymbol{\Psi}(\theta_{i,j}) \in \mathbb{C}^U$. A suitable basis for 2D is given by the Fourier functions

$$\boldsymbol{\Psi}(\theta_{i,j}) = \begin{bmatrix} \frac{1}{\sqrt{2\pi}} e^{\mathrm{j}\theta_{i,j}[\boldsymbol{u}]_1} & ... & \frac{1}{\sqrt{2\pi}} e^{\mathrm{j}\theta_{i,j}[\boldsymbol{u}]_U} \end{bmatrix}^T \quad (12)$$

with $\boldsymbol{u} = \left[\left\lfloor -\frac{U-1}{2} \right\rfloor, ..., \left\lfloor \frac{U-1}{2} \right\rfloor \right]^T$. An extension of the basis to azimuth and elevation is possible, but beyond the scope of this paper. It is known that $|[\boldsymbol{G}]_{m,u}|$ decays superexponentially for increasing u beyond $u = kr$, where k is the angular wavenumber and r the radius of the smallest sphere enclosing the antenna [11]. Therefore a low order U is sufficient to obtain an accurate representation of the antenna response vector. With spatial samples from antenna calibration measurements or EMF simulation, $\boldsymbol{G}$ can be determined by least squares.

ISBN 978-90-827970-1-5 © EURASIP 2018

Having obtained the sampling matrix, it can be used to interpolate the antenna response vector $\boldsymbol{a}(\theta_{i,j})$ and determine the CRB for real antennas in closed form.

In Section III, we show the position and orientation estimation bounds for an MMA [3], [4]. It is a single patch antenna with four ports having different antenna power patterns different phase responses. The sampled and interpolated power patterns can be seen in Figure 2. Both power and phase contain position and orientation information which needs to be considered for the derivation of the fundamental limits.

C. Fisher Information Matrix

We assess the fundamental limits for joint orientation and position estimation in terms of Fisher information. For circular symmetric Gaussian noise $w_{i,j}^m$, the Fisher information matrix (FIM) can be calculated by [14],

$$\boldsymbol{I} = \frac{2}{\sigma^2}\,\mathrm{Re}\left\{\sum_{n=0}^{N-1}\frac{\partial E[\boldsymbol{r}(n)]^H}{\partial[\boldsymbol{\xi}^T\ \boldsymbol{\eta}^T]^T}\frac{\partial E[\boldsymbol{r}(n)]}{\partial[\boldsymbol{\xi}^T\ \boldsymbol{\eta}^T]^T}\right\}. \tag{13}$$

The FIM $\boldsymbol{I} \in \mathbb{R}^{(3K+2L)\times(3K+2L)}$ is structured into four blocks,

$$\boldsymbol{I} = \frac{2}{\sigma^2}\begin{bmatrix}\boldsymbol{I}_{\boldsymbol{\xi}} & \boldsymbol{I}_{\boldsymbol{\xi\eta}}\\ \boldsymbol{I}_{\boldsymbol{\xi\eta}}^H & \boldsymbol{I}_{\boldsymbol{\eta}}\end{bmatrix} \tag{14}$$

with $\boldsymbol{I}_{\boldsymbol{\xi}} \in \mathbb{R}^{3K\times 3K}$, $\boldsymbol{I}_{\boldsymbol{\xi\eta}} \in \mathbb{R}^{3K\times 2L}$ and $\boldsymbol{I}_{\boldsymbol{\eta}} \in \mathbb{R}^{2L\times 2L}$.

The upper-left part $\boldsymbol{I}_{\boldsymbol{\xi}}$ corresponds to the agent unknowns. Having K agents, it consists of K sub-matrices with dimension 3x3, given by

$$\begin{aligned}[\boldsymbol{I}_{\boldsymbol{\xi}}]_{u,v} &= \sum_{(i,j)\in\mathbb{L}}\sum_{m=0}^{M-1}\sum_{n=0}^{N-1}\mathrm{Re}\left\{\frac{\partial E[r_{i,j}^m(n)]^*}{\partial \boldsymbol{\xi}_u^T}\frac{\partial E[r_{i,j}^m(n)]}{\partial \boldsymbol{\xi}_v}\right\}\\ &= \sum_{(i,j)\in\mathbb{L}}\sum_{m=0}^{M-1}\sum_{n=0}^{N-1}\\ &\quad\mathrm{Re}\left\{\begin{bmatrix}\frac{\partial E[r_{i,j}^m(n)]^*}{\partial \boldsymbol{p}_u^T}\frac{\partial E[r_{i,j}^m(n)]}{\partial \boldsymbol{p}_v} & \frac{\partial E[r_{i,j}^m(n)]^*}{\partial \boldsymbol{p}_u^T}\frac{\partial E[r_{i,j}^m(n)]}{\partial \psi_v}\\ \frac{\partial E[r_{i,j}^m(n)]^*}{\partial \psi_u}\frac{\partial E[r_{i,j}^m(n)]}{\partial \boldsymbol{p}_v} & \frac{\partial E[r_{i,j}^m(n)]^*}{\partial \psi_u}\frac{\partial E[r_{i,j}^m(n)]}{\partial \psi_v}\end{bmatrix}\right\}\end{aligned} \tag{15}$$

Using the observation that $\frac{\partial E[r_{i,j}^m(n)]}{\partial \boldsymbol{\xi}_u} = 0$ for $u \neq i \wedge u \neq j$; $\frac{\partial E[r_{j,i}^m(n)]}{\partial \boldsymbol{p}_i} = -\frac{\partial E[r_{j,i}^m(n)]}{\partial \boldsymbol{p}_j}$ and $\frac{\partial E[r_{j,i}^m(n)]}{\partial \psi_i} = 0$, the sub-matrices on the diagonal simplify to

$$\begin{aligned}[\boldsymbol{I}_{\boldsymbol{\xi}}]_{i,i} &= \sum_{j\in\mathbb{L}_i}\sum_{m=0}^{M-1}\sum_{n=0}^{N-1}\\ &\quad\mathrm{Re}\left\{\begin{bmatrix}A & \frac{\partial E[r_{i,j}^m(n)]^*}{\partial \boldsymbol{p}_i^T}\frac{\partial E[r_{i,j}^m(n)]}{\partial \psi_i}\\ \frac{\partial E[r_{i,j}^m(n)]^*}{\partial \psi_i}\frac{\partial E[r_{i,j}^m(n)]}{\partial \boldsymbol{p}_i} & \left|\frac{\partial E[r_{i,j}^m(n)]}{\partial \psi_i}\right|^2\end{bmatrix}\right\}\\ &= E_s\alpha_{i,j}^2\sum_{j\in\mathbb{L}_u}\sum_{m=0}^{M-1}\\ &\quad\begin{bmatrix}B & -\left|\frac{\partial a^m(\theta_{i,j})}{\partial\theta_{i,j}}\right|^2\frac{\partial\theta_{i,j}}{\partial \boldsymbol{p}_i^T}\\ -\left|\frac{\partial a^m(\theta_{i,j})}{\partial\theta_{i,j}}\right|^2\frac{\partial\theta_{i,j}}{\partial \boldsymbol{p}_i} & \left|\frac{\partial a^m(\theta_{i,j})}{\partial\theta_{i,j}}\right|^2\end{bmatrix},\end{aligned} \tag{16}$$

with

$$A = \frac{\partial E[r_{i,j}^m(n)]^*}{\partial \boldsymbol{p}_i^T}\frac{\partial E[r_{i,j}^m(n)]}{\partial \boldsymbol{p}_i} + \frac{\partial E[r_{j,i}^m(n)]^*}{\partial \boldsymbol{p}_j^T}\frac{\partial E[r_{j,i}^m(n)]}{\partial \boldsymbol{p}_j}, \tag{17}$$

$$\begin{aligned}B &= \left|\frac{\partial a^m(\theta_{i,j})}{\partial\theta_{i,j}}\right|^2\frac{\partial\theta_{i,j}}{\partial \boldsymbol{p}_i^T}\frac{\partial\theta_{i,j}}{\partial \boldsymbol{p}_i} + \overline{f^2}|a^m(\theta_{i,j})|^2\frac{\partial\tau_{i,j}}{\partial \boldsymbol{p}_i^T}\frac{\partial\tau_{i,j}}{\partial \boldsymbol{p}_i}\\ &\quad + \left|\frac{\partial a^m(\theta_{j,i})}{\partial\theta_{j,i}}\right|^2\frac{\partial\theta_{j,i}}{\partial \boldsymbol{p}_j^T}\frac{\partial\theta_{j,i}}{\partial \boldsymbol{p}_j} + \overline{f^2}|a^m(\theta_{j,i})|^2\frac{\partial\tau_{j,i}}{\partial \boldsymbol{p}_j^T}\frac{\partial\tau_{j,i}}{\partial \boldsymbol{p}_j},\end{aligned} \tag{18}$$

where the signal energy E_s is given by (23) and the mean square bandwidth $\overline{f^2}$ by (25). The off-diagonal blocks are

$$\begin{aligned}[\boldsymbol{I}_{\boldsymbol{\xi}}]_{i,j} &= \sum_{m=0}^{M-1}\sum_{n=0}^{N-1}\\ &\quad\mathrm{Re}\left\{\begin{bmatrix}-A & -\frac{\partial E[r_{j,i}^m(n)]^*}{\partial \boldsymbol{p}_j^T}\frac{\partial E[r_{j,i}^m(n)]}{\partial \psi_j}\\ -\frac{\partial r_{i,j}^m(n)^*}{\partial \psi_i}\frac{\partial r_{i,j}^m(n)}{\partial \boldsymbol{p}_i} & 0\end{bmatrix}\right\}\\ &= E_s\alpha_{i,j}^2\sum_{m=0}^{M-1}\begin{bmatrix}-B & \left|\frac{\partial a^m(\theta_{j,i})}{\partial\theta_{j,i}}\right|^2\frac{\partial\theta_{j,i}}{\partial \boldsymbol{p}_j^T}\\ \left|\frac{\partial a^m(\theta_{i,j})}{\partial\theta_{i,j}}\right|^2\frac{\partial\theta_{i,j}}{\partial \boldsymbol{p}_i} & 0\end{bmatrix}.\end{aligned} \tag{19}$$

The upper-right part $\boldsymbol{I}_{\boldsymbol{\xi\eta}}$ relates agent and link unknowns and consists of 3x2 blocks. For the i-th block row, referring to agent i, we have

$$\begin{aligned}[\boldsymbol{I}_{\boldsymbol{\xi\eta}}]_{i,(i,j)} &= \sum_{m=0}^{M-1}\mathrm{Re}\left\{E_s\alpha_{i,j}\frac{\partial a^m(\theta_{i,j})^*}{\partial\theta_{i,j}}a^m(\theta_{i,j})\right.\\ &\qquad\left.\begin{bmatrix}\frac{\partial\theta_{i,j}}{\partial \boldsymbol{p}_i^T} & j\alpha_{i,j}\frac{\partial\theta_{i,j}}{\partial \boldsymbol{p}_i^T}\\ -1 & -j\alpha_{i,j}\end{bmatrix}\right\},\end{aligned} \tag{20}$$

and accordingly for block-row of agent j

$$\begin{aligned}[\boldsymbol{I}_{\boldsymbol{\xi\eta}}]_{j,(i,j)} &= \sum_{m=0}^{M-1}\mathrm{Re}\left\{E_s\alpha_{i,j}\frac{\partial a^m(\theta_{i,j})^*}{\partial\theta_{i,j}}a^m(\theta_{i,j})\right.\\ &\qquad\left.\begin{bmatrix}-\frac{\partial\theta_{i,j}}{\partial \boldsymbol{p}_i^T} & -j\alpha_{i,j}\frac{\partial\theta_{i,j}}{\partial \boldsymbol{p}_i^T}\\ 0 & 0\end{bmatrix}\right\}.\end{aligned} \tag{21}$$

The lower-right part $\boldsymbol{I}_{\boldsymbol{\eta}}$ corresponds to the link unknowns. Since $\mathrm{Re}\left\{\frac{\partial E[r_{i,j}^m(n)]^*}{\partial\phi_{i,j}}\frac{\partial E[r_{i,j}^m(n)]}{\partial\alpha_{i,j}}\right\} = 0$, it is a diagonal matrix

$$\boldsymbol{I}_{\boldsymbol{\eta}} = \sum_{m=0}^{M-1}E_s\left|a^m(\theta_{i,j})\right|^2\mathrm{diag}\left\{\begin{bmatrix}\ldots & 1 & \alpha_{i,j}^2 & \ldots\end{bmatrix}\right\}. \tag{22}$$

The partial derivatives of the signal always show up as conjugate products, see (13). Like that, three different inner products of the signal or its derivative appear. The first one is the signal energy of the OFDM signal

$$E_s = \sum_{n=0}^{N-1}|s(nT-\tau_{i,j})|^2 = \sum_{q=\lfloor-\frac{N-1}{2}\rfloor}^{\lfloor\frac{N-1}{2}\rfloor}|S_q|^2, \tag{23}$$

ISBN 978-90-827970-1-5 © EURASIP 2018

The cross-term

$$\sum_{n=0}^{N-1} s(nT-\tau_{i,j})^* \frac{\partial s(nT-\tau_{i,j})}{\partial \tau_{i,j}} = 0. \tag{24}$$

The third one is related to the mean-square bandwidth [14], which is a measure of the ranging capability of a signal. For OFDM signals it is given by [12]

$$\overline{f^2} = \frac{1}{E_s}\sum_{n=0}^{N-1}\left|\frac{\partial s(nT-\tau_{i,j})}{\partial \tau_{i,j}}\right|^2 = \frac{4\pi^2 f_{\mathrm{sc}}^2}{E_s}\sum_{q=\lfloor -\frac{N-1}{2}\rfloor}^{\lfloor \frac{N-1}{2}\rfloor} q^2|S_q|^2. \tag{25}$$

D. Position and Orientation Error Bound

Having constructed the FIM, the CRB for position and orientation can be obtained by applying Schur complement,

$$\mathrm{COV}[\hat{\boldsymbol{\xi}}] \succcurlyeq \mathrm{CRB}[\boldsymbol{\xi}] = \frac{\sigma^2}{2}\left(\boldsymbol{I}_{\boldsymbol{\xi}} - \boldsymbol{I}_{\boldsymbol{\xi\eta}}\boldsymbol{I}_{\boldsymbol{\eta}}^{-1}\boldsymbol{I}_{\boldsymbol{\xi\eta}}^{H}\right)^{\dagger}, \tag{26}$$

where † denotes the Moore-Penrose pseudoinverse and $U \succcurlyeq V$ means $U - V$ is positive semidefinite [15]. As we consider relative positioning, the FIM is always rank deficient by three, corresponding to one rotational and two translational degrees of freedom. Hence the regular inverse does not exist. Taking the pseudoinverse inherently assumes that an optimal coordinate system is chosen for relative positioning [15]. Other sub-optimal choices would lead to an increase of the CRB.

The bound on the covariance of the position estimate for one agent can be assessed by extracting the corresponding 2x2 submatrix,

$$\mathrm{COV}[\hat{\boldsymbol{p}}_i] \succcurlyeq \mathrm{CRB}[\boldsymbol{p}_i] = \begin{bmatrix} [\mathrm{CRB}[\boldsymbol{\xi}]]_{3i,3i} & [\mathrm{CRB}[\boldsymbol{\xi}]]_{3i,3i+1} \\ [\mathrm{CRB}[\boldsymbol{\xi}]]_{3i+1,3i} & [\mathrm{CRB}[\boldsymbol{\xi}]]_{3i+1,3i+1} \end{bmatrix} \tag{27}$$

Applying eigenvalue decomposition,

$$\mathrm{COV}[\hat{\boldsymbol{p}}_i] = R\begin{bmatrix}\lambda_1^2 & 0\\ 0 & \lambda_2^2\end{bmatrix}R^T \tag{28}$$

we can interpret the result as an ellipse with major axis λ_1 and minor axis λ_2 rotated by the rotation matrix R.

The variance of the orientation estimate is lower bounded by

$$\mathrm{VAR}[\hat{\psi}_i] \geq \mathrm{CRB}[\psi_i] = [\mathrm{CRB}[\boldsymbol{\xi}]]_{3i+2,3i+2}. \tag{29}$$

III. Results

In this section we present results for an MMA prototype [3], [4], which is a special type of directive patch antenna with 4 ports, see Figure 2. To obtain omni-directional coverage, we assume three of these antennas are mounted vertically on top of each rover with 60° angle in between, see Figure 1. Only one of the MMAs is active at a time and we assume a-priori knowledge of the correct antenna for each link. In practice, this could be done e.g. by a simple decision based on the received signal power. We assume a bandwidth of 25 MHz and $N = 1024$ subcarriers, resulting in a subcarrier spacing of $f_{\mathrm{sc}} = 24.41\,\mathrm{kHz}$. To setup a noise level, we assume $-5\,\mathrm{dBm}$ transmit power, a receiver temperature of 290 K, an additional noise figure of 8 dB and free-space path loss for $f_c = 5.2\,\mathrm{GHz}$. Figure 3 shows the 300-sigma position error bound ellipses and the 300-sigma orientation error bound sectors for all agents. 300-sigma was chosen to allow a graphical representation for the given scenario. The agent in the bottom left, which is more remote and has fewer connections than the other agents, clearly has the highest bounds. For the other agents, the bounds are similar.

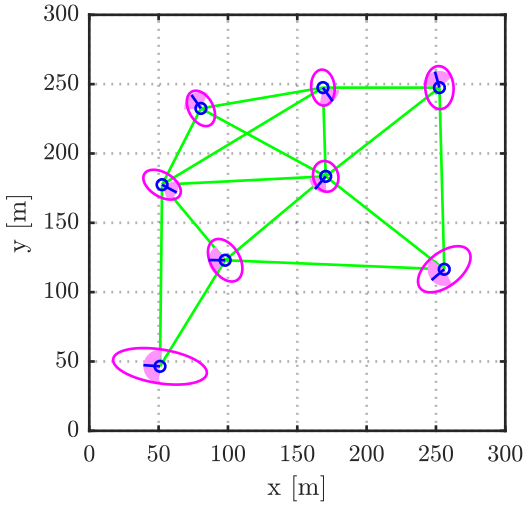

Fig. 3. Position (ellipse) and orientation (sector) error bound.

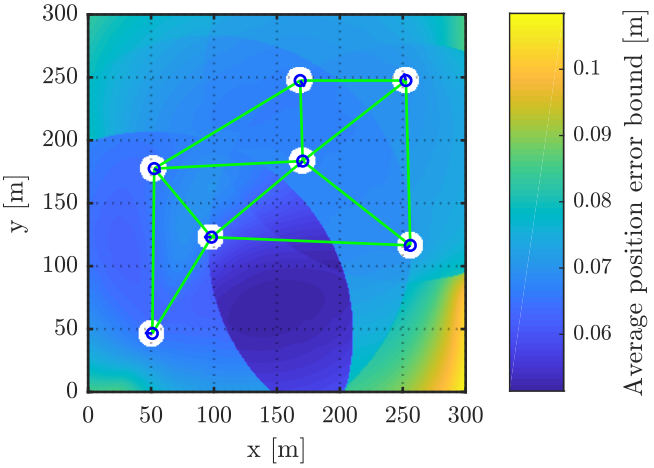

Fig. 4. Average position error bound of the swarm when moving one agent to different positions.

The derived CRB can not only be used to assess limits for a given formation, but also for swarm deployment and control. As an example we move the top-left agent from Figure 1 to all possible positions and calculate the CRB averaged over all agents. A receiver sensitivity corresponding to a maximum distance of 160 m is assumed. The minimum distance between the agents is 10 m to avoid collisions and to ensure far-field conditions. Figure 4 shows the average position error bound of the swarm $\sqrt{\frac{1}{K}\sum_{i=1}^{K}\mathrm{tr}[\mathrm{CRB}[\boldsymbol{p}_i]]}$, when the agent is moved to the corresponding position. The lowest position error bound

ISBN 978-90-827970-1-5 © EURASIP 2018

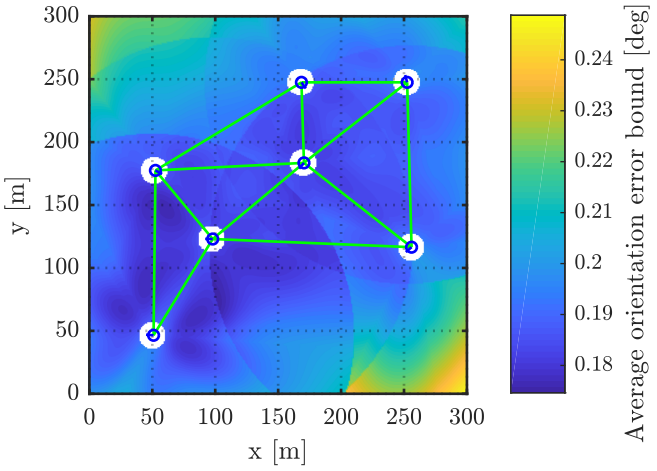

Fig. 5. Average orientation error bound of the swarm when moving one agent to different positions.

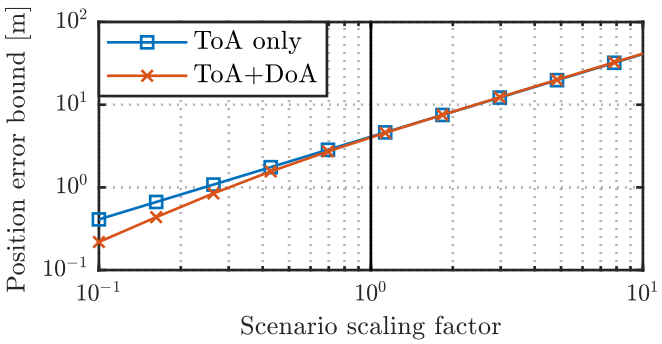

Fig. 6. ToA only and combined ToA+DoA position error bounds for the scenario shown in Figure 3, scaled in size by a variable factor.

can be achieved if the agent is placed around point [150 70]. Accordingly, Figure 5 shows the average orientation error bound $\sqrt{\frac{1}{K}\sum_{i=1}^{K}\mathrm{CRB}[\psi_i]}$, which does not vary much as long as the agent is not moved too far away. Apparently, orientation is less critical than position estimation for this scenario. This also proves that the chosen setup with three MMAs on each agent is feasible for joint position and orientation estimation.

Having ToA and DoA information available, both are used for positioning. Figure 6 compares ToA only with ToA+DoA for the scenario shown in Figure 3. The plot reveals that DoA brings a benefit for positioning at short distances. It has to be stressed that this result is scenario specific. Relative positioning with DoA information only is not possible, because the solution always contains a scaling degree of freedom. This corresponds to a rank decrease of the FIM by one.

IV. Conclusion

In this paper we have derived the fundamental limits in terms of the CRB for joint relative position and orientation estimation. In the literature, fundamental limits for joint position and orientation estimation can be found. However, they do not cover the relative, i.e. anchor-free, case and are limited to ideal antenna arrays like ULA or UCA. In contrast to that, we employ wavefield modeling and manifold separation to yield a bound for real multi-port antenna systems by incorporating calibration or EMF simulation data. As an example, we show bounds for a multi-agent system featuring MMAs. Additionally, we examine where to move an agent such that it is most beneficial for position and orientation estimation. It is found that positioning is much more sensitive to the position of the agent than orientation estimation. Finally we discuss that DoA information brings a benefit for positioning only at short distances, whereas ToA is crucial for relative positioning.

Acknowledgment

This work has been funded by the German Research Foundation (DFG) under contract numbers FI 2176/1-1 and HO 2226/17-1.

References

[1] S. Zhang, E. Staudinger, S. Sand, R. Raulefs, and A. Dammann, "Anchor-free localization using round-trip delay measurements for martian swarm exploration," in *2014 IEEE/ION Position, Location and Navigation Symposium-PLANS 2014*. IEEE, 2014, pp. 1130–1139.

[2] S. Zhang, R. Raulefs, and A. Dammann, "Location information driven formation control for swarm return-to-base application," in *2016 24th European Signal Processing Conference (EUSIPCO)*, Aug. 2016, pp. 758–763.

[3] R. Pöhlmann, S. Zhang, Yinusa, Kazeem A., and A. Dammann, "Multimode antenna specific direction-of-arrival estimation schemes," in *2017 IEEE 7th International Workshop on Computational Advances in Multi-Sensor Adaptive Processing (CAMSAP)*, Curacao, Dec. 2017, pp. 462–466.

[4] D. Manteuffel and R. Martens, "Compact Multimode Multielement Antenna for Indoor UWB Massive MIMO," *IEEE Transactions on Antennas and Propagation*, vol. 64, no. 7, pp. 2689–2697, Jul. 2016.

[5] Y. Shen, H. Wymeersch, and M. Z. Win, "Fundamental limits of wideband localization—Part II: Cooperative networks," *IEEE Transactions on Information Theory*, vol. 56, no. 10, pp. 4981–5000, 2010.

[6] C. Chang and A. Sahai, "Cramér-Rao-type bounds for localization," *EURASIP Journal on Advances in Signal Processing*, vol. 2006, no. 1, Dec. 2006.

[7] D. C. Popescu, M. Hedley, and T. Sathyan, "Posterior Cramér-Rao Bound for anchorless tracking," *IEEE Signal Processing Letters*, vol. 20, no. 12, pp. 1183–1186, Dec. 2013.

[8] A. Shahmansoori, G. E. Garcia, G. Destino, G. Seco-Granados, and H. Wymeersch, "5G position and orientation estimation through millimeter wave MIMO," in *2015 IEEE Globecom Workshops (GC Wkshps)*, Dec. 2015, pp. 1–6.

[9] A. Guerra, F. Guidi, and D. Dardari, "Position and orientation error bound for wideband massive antenna arrays," in *2015 IEEE International Conference on Communication Workshop (ICCW)*, Jun. 2015, pp. 853–858.

[10] Y. Shen and M. Z. Win, "Fundamental limits of wideband localization—Part I: A general framework," *IEEE Transactions on Information Theory*, vol. 56, no. 10, pp. 4956–4980, 2010.

[11] M. A. Doron and E. Doron, "Wavefield modeling and array processing. I. Spatial sampling," *IEEE Transactions on Signal Processing*, vol. 42, no. 10, pp. 2549–2559, 1994.

[12] S. Sand, A. Dammann, and C. Mensing, *Positioning in Wireless Communications Systems*. John Wiley & Sons, Feb. 2014.

[13] M. Costa, A. Richter, and V. Koivunen, "DoA and polarization estimation for arbitrary array configurations," *IEEE Transactions on Signal Processing*, vol. 60, no. 5, pp. 2330–2343, May 2012.

[14] S. M. Kay, *Fundamentals of Statistical Signal Processing, Volume I: Estimation Theory*, 1st ed. Englewood Cliffs, N.J: Prentice Hall, Apr. 1993.

[15] J. N. Ash and R. L. Moses, "On the relative and absolute positioning errors in self-localization systems," *IEEE Transactions on Signal Processing*, vol. 56, no. 11, pp. 5668–5679, Nov. 2008.

ISBN 978-90-827970-1-5 © EURASIP 2018